

Stabilization of sawteeth instability by short gas pulse injection in ADITYA-U tokamak

Suman Dolui^{1,2}, Kaushlender Singh^{1,2}, Bharat Hegde^{1,2}, T. Macwan³, SK Injamul Hoque^{1,2}, Umesh Nagora^{1,2}, Jaya Kumar A.⁴, S. Purohit¹, A. N. Adhiya¹, K. A. Jadeja¹, Harshita Raj^{1,2}, Ankit Kumar^{1,2}, Ashok K. Kumawat^{1,2}, Suman Aich^{1,2}, Rohit Kumar¹, K. M. Patel¹, P. Gautam¹, Sharvil Patel¹, N. Yadava⁵, N. Ramaiya¹, M. K. Gupta¹, S. K. Pathak^{1,2}, M. B. Chowdhuri¹, S. Sharma^{1,2}, A. Kuley⁴, R. L. Tanna¹, P. K. Chattopadhyay^{1,2}, A. Sen^{1,2}, Y. C. Saxena^{1,2}, R. Pal⁶ and Joydeep Ghosh^{1,2}

¹*Institute for Plasma Research, Gandhinagar 382 428*

²*Homi Bhabha National Institute, Anushaktinagar, Mumbai 400094, India*

³*Department of Physics and Astronomy, University of California Los Angeles, Los Angeles, California 90095, USA*

⁴*Department of Physics, Indian Institute of Science, Bangalore-560012, India*

⁵*Oak Ridge Associated Universities, Oak Ridge 37831, USA*

⁶*Saha Institute of Nuclear Physics, Kolkata 700064, India*

Experiments on ADITYA-U tokamak show a marked enhancement in the sawtooth period by application of short gas-puffs of fuel that cause a modification of the radial density profile. A consequent suppression of the trapped electron modes (TEMs) then leads to an increase in the core electron temperature. This slows down the heat propagation following a sawtooth crash causing a delay in achieving the critical temperature gradient inside the $q = 1$ surface required for the next sawtooth crash to happen. The overall scenario has strong similarities with the behavior of sawtooth under electron cyclotron resonance heating (ECRH). Our findings suggest an alternate, simpler technique for sawtooth control that may be usefully employed in small/medium sized tokamaks that do not have an ECRH or any other auxiliary heating facility.

Sawtooth oscillation in a tokamak plasma is a quasi-periodic phenomenon where electron temperature gradually rises in the core region followed by a sudden crash via internal disruption [1] [2]. The phenomenon is detrimental to heating and particle confinement in the core of the plasma. The sawtooth-crash also leads to generation of instabilities affecting the steady-state scenario [3] [4] of fusion grade plasmas. Therefore, the disruption needs to be controlled; though, its complete suppression is not desirable, as it can lead to impurity peaking which causes substantial degradation of confinement [5]. A controlled stabilization is thus ideally desirable to proceed towards the fusion reactor goal. The sawtooth crash is attributed to magnetic relaxation by Kadomtsev's well-known resistive reconnection model [6], which considers excitation and nonlinear growth of a $m/n=1/1$ internal kink or tearing mode near the $q = 1$ surface (m and n are poloidal and toroidal mode numbers, respectively and q , the safety factor, is a measure of the helicity of the magnetic field) to be the cause behind the internal disruption. The model predicts crash times that agree well with several tokamaks but predicts much larger crash time than that observed ($\sim 100\mu\text{S}$) in large tokamaks. Furthermore, the mode oscillations are not always observed before the crash. So, understanding sawtooth relaxation remains an open question, and deserves further studies to control it effectively. Several models have been proposed to explore possible mechanisms for the stabilization: some are based on controlling the fast particles generated during heating mechanisms to lower the pressure gradient, while others depend on decreasing the

magnetic shear near the $q=1$ region [7]. It has been conjectured that the growth rate of the $m/n = 1/1$ mode can be influenced by the presence of energetic ions [8] [9], or by intrinsic plasma rotation [10], or by shear in rotation [9] [11]. Dynamic modification of plasma parameters near $q=1$ surface seems to be crucial to prevent the crash. Experimentally, localized heating by lower-hybrid current drive, ion-cyclotron resonance heating, electron cyclotron resonance (ECR) heating and neutral beam heating [8] [12], have demonstrated substantial control of the sawtooth destabilization. Recent experiment in DIII-D tokamak [13] using ECR heating suggests the temperature turbulence inside the inversion radius (a radius beyond which the sawtooth character reverses) is involved in triggering the sawtooth crash. In this Letter, we present employment of a successful alternate scheme that experimentally demonstrate delaying the sawtooth crash substantially in ADITYA-U tokamak, by controlling the plasma temperature profile inside the $q=1$ surface. The scheme involves injection of short puffs of fuel-gas (containing around $\sim 10^{17}$ - 10^{18} molecules/ m^3) in the plasma edge. The injection results in a cold-pulse propagation [14] [15] [16] which modifies the radial profile of plasma density in the mid-radius region and subsequently modifies the electron temperature profile in the core region (inside $q=1$ surface). The observed sawtooth stabilization results closely resemble those obtained through localized ECR heating near the $q=1$ surface in DIII-D tokamak [17]. So, the present mechanism provides a relatively simpler technique for studying sawtooth phenomena systematically in tokamaks. The

present experiment is conducted in the Ohmically-heated hydrogen discharges of the ADITYA-U tokamak [18] with toroidal magnetic field $B_\phi = 1.2-1.4$ T and plasma current $I_p = 150-180$ kA. The plasma major radius $R = 0.75$ m and a toroidal-belt limiter defines the minor radius, a , to be 0.25 m. The central chord-averaged electron density (\bar{n}_e) and electron temperature (T_e) are $1 - 4 \times 10^{19} m^{-3}$ and 200-350 eV, respectively. The radial density profile is measured using a seven-channel (3 heterodyne + 4 homodyne) microwave interferometer [19], whereas the core electron temperature is obtained by soft-X-ray (SXR) emission measurements using foil-ratio method [20]. A SXR tomography camera, consisting of 16-channel AXUV photodiodes, scans the radius from $r = -10$ to 10 cm [21]. The edge density and temperature are measured by Langmuir probes [22]. The locations of various diagnostics and gas-puff injection point are described in Ref. 14. Figure 1 shows a typical discharge evolution of the parameters I_p , loop-voltage V_{loop} , central chord-averaged SXR emission and density \bar{n}_e with the application of periodic hydrogen/deuterium gas-puffs. The amount of gas injection is controlled by varying the voltage pulse width to the piezo-valve; a pulse width of ~ 1 ms injects $\sim 10^{17}$ molecules [14]. The sawtooth activities are observed in various parameters including the SXR emission from the central chord (Figure 1a).

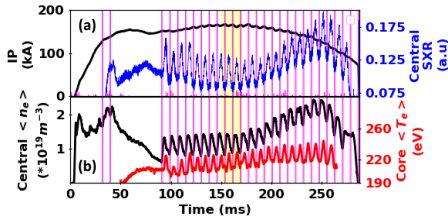


Figure 1: Temporal evolution of plasma parameters (Shot # 33689); (a) I_p (black), SXR emission (blue), (b) Central chord integrated density n_e (black); Core T_e (red)

The sawtooth cycle shows a quiescent ramp phase ($\sim 600 \mu s$), followed by a crash ($\sim 50-100 \mu s$). The peak corresponds to ~ 10 % rise in core plasma temperature T_{e0} . The sawtooth inversion radius is $r_{inv} \sim 4-6$ cm. Taking $T_{e0} \sim 300$ eV and core density $n_{e0} \sim 2 \times 10^{19} m^{-3}$, in these discharges, the observed sawtooth crash-time, is close to the characteristic Sweet-Parker time scale $\sqrt{\tau_R \tau_A} \sim 85 \mu s$, where $\tau_A = r_{inv} \sqrt{4\pi \rho_m B_\phi^{-1}}$, $\tau_R = 4\pi r_{inv}^2 / \eta c^2$, ρ_m is the mass density, η is the plasma resistivity.

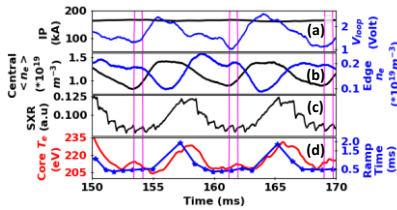


Figure 2: Temporal evolution of (a) I_p (black), V_{loop} (blue) (b) $n_e >$ (black), edge n_e (blue) (c) central chord SXR intensity (black) (d) core T_e (red solid line), Ramp time of sawteeth cycle (blue stars) (Shot # 33689).

To examine the sawtooth activity closely, the time span 150-170 ms during the plasma current flat-top is expanded in Figure 2. Impact of the gas pulse injection (done repeatedly at 8 ms intervals) is clearly visible on the sawtooth oscillations in SXR intensity (Figure 2c), as well as on I_p , V_{loop} , \bar{n}_e , n_e^{edge} (at $r = 24$ cm) and T_{e0} . The most interesting point to note here is that the ramp phase is extended substantially after each gas-puff and the crash is delayed. The ramp time of each cycle is plotted in Figure 2d. After each gas-puff the ramp time is increased to nearly 1 - 1.5 ms, which is about double the time compared to that seen without gas-puff. The increment in the ramp time gradually decreases in subsequent sawtooth pulses and attains the pre-gas-puff value after 3-4 cycles depending on the amount of gas injected. The results are confirmed by repeated observations over several tens of discharges covering hundreds of sawtooth cycles. The increment in sawtooth ramp-time is seen to rise proportional to the amount of gas injected until it affects the plasma adversely (Figure 3).

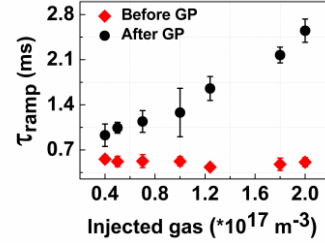


Figure 3: Ramp time of sawtooth cycle (black circle) with amount of injected gas. Corresponding ramp time in absence of gas-puff (red triangle).

As shown in Figure 2b, following the gas-pulse injection, \bar{n}_e increases sharply, and reaches a peak in about 1 ms after the injected pulse, whereas the edge plasma density (at $\rho=r/a \sim 0.8-1$) decreases. The temperature of the core plasma also increases (Figure 2d); however, it starts rising later, near about the time the density enhancement reaches its peak. The temperature rise time to the peak is 2-3 ms, which is smaller than the energy confinement time (~ 5 ms). The above observations clearly suggest a cold pulse propagation phenomenon by the gas-puff. The SXR emission remains confined within the core region of the plasma ($\rho < 0.3$ in this experiment), where the electron temperature is more than 100-200 eV. The SXR emission intensity is known to be proportional to n_e^2 , but more sensitive to T_e . In the experiment, the temporal evolution of the gas-puff induced SXR emission (Figure 2c) closely follows the core temperature variation (Figure 2d), rather than the density variation (Figure 2b). This clearly indicates the gas puff affects the temperature in the core region, where the density does not change

much. Experimental results shown below in Figure 4 are consistent with this proposition. In Figure 4(a), we compare the radial profiles of density with and without gas puff. After gas injection the density does not change much inside, but increases considerably outside the core ($\rho > 0.3$) of the plasma. In other words, the density profile is flattened by the gas-puff. The maximum density increment is observed at about 1 ms after the gas injection between $\rho = 0.4 - 0.6$, indicating the density to change mainly outside the SXR emission zone.

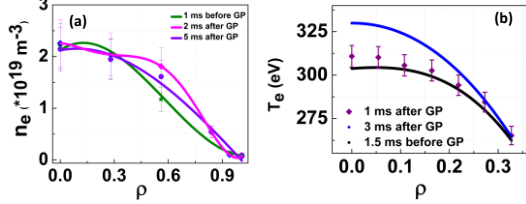


Figure 4: (a) Radial profile of density and (b) radial profile of core T_e before and after gas-puff. The curves are the spline fits to the experimental data (symbol)

In contrast, radial temperature profiles (Figure 4b), show the temperature to rise in the core region. The sign inversion of temperature increment occurs in the vicinity of the $q=1$ surface, pointing towards the profile to become more peaked after the gas puff. The above observations resemble those observed in the cold pulse propagation phenomenon in DIII-D and ASDEX Upgrade tokamaks caused by impurity-injection. They have been successfully explained by a model [15] which predicts that flattening of the electron density profile stabilizes the Trapped Electron Mode (TEM) instability, thereby leads to turbulence reduction [23][15] and reduced transport, if the heat transport is dominated by electron heat flux. To identify whether electron or ion scale turbulences are involved here, self-consistent gyrokinetic simulations [24] are conducted for the present ADITYA-U discharges using the GTC code for cases before and after gas pulse injection, incorporating the equilibrium profiles obtained through IPR-EQ code [25]. The primary feature of the linear eigenmode structure, which propagates in the electron diamagnetic direction with $k_{\perp}\rho_i \sim 0.7$, is identified as a trapped electron-driven instability (TEM) [26][23] and which plays a significant role in generating the anomalous turbulent transport. In linear regime, the TEM turbulence structure shows a relatively larger radial extent on the low-field side before gas injection; whereas, with gas-puff, it contracts with the turbulence peak moving outwards (shown in Figure 5b). In nonlinear regime, however, the turbulence encompasses almost the entire plasma ($\rho = 0.1-1$) with no gas injection; whereas, with gas injection it is suppressed in a broad region (up to $\rho \sim 0.25$, i.e. near to $q=1$ surface) of the core plasma (Figure 5b) and it is clearly depicted in the poloidal plane plot of Figure 5a. It is plausible that such fluctuation

suppression with gas-puff causes reduction of heat transport from a broader region, and is likely to produce gradual rise of core temperature for a longer time to a significant level. This is manifested also in the observed temperature profile of Figure 4b. The region near the magnetic axis is excluded in the simulations, since no turbulence activity exists there. The observations are very much similar to those obtained with temperature modification experiments near the $q=1$ surface by ECR or LH heating. The sawtooth cycle before gas-puff shows a gradual increase in the SXR emission until a growing

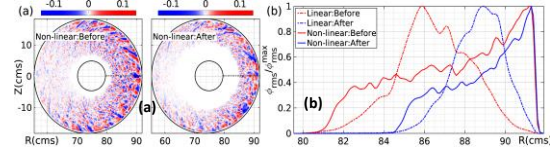


Figure 5: (a) Electrostatic perturbed potential on the poloidal plane during the nonlinear phase and (b) the corresponding radial variation of the rms electrostatic potential normalized with the maximum values during the linear and nonlinear phase.

precursor oscillation (oscillation period $\sim 50 \mu\text{s}$) develops on it followed by a crash. After gas-puff, similar precursor oscillation develops, but not before a substantial delay. The SXR emissions along two chords on either side of the center are plotted in Figure 6. In both the cases, the precursor oscillation grows in amplitude until the crash, however, the oscillation survives the crash and stays as a steady level (Figure 6d). Detailed analysis of the oscillation (Figure 6c) distinctly shows 180° phase difference between them indicating an odd m mode (most likely $m=1$). In our experiments, taking the plasma parameters of the core, the ideal $m=1$ kink mode is considered stable [27]. Hence, the observed $m=1$ oscillation may be due to excitation of a resistive mode producing a slowly growing island. The survival of the oscillations supports partial reconnection during the sawtooth phase. Incomplete reconnection has been described by several models [31]. These include a flattened q profile, shear flow, stochastic magnetic fields [32], diamagnetic suppression of the nonlinear internal kink mode [7], pressure effects at the magnetic island boundary, etc.

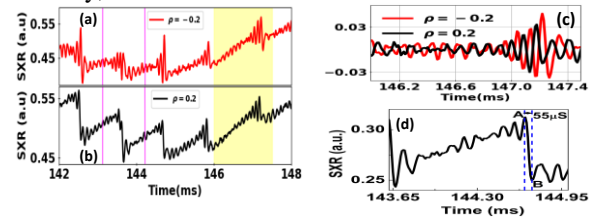


Figure 6: SXR intensity at (a) $\rho = 0.20$ and (b) $\rho = -0.20$. (c) SXR fluctuations at $\rho = 0.20$ (black) and $\rho = -0.20$ (red). (d) A typical sawtooth crash phase with presence of pre and post cursor oscillations.

The Kadomtsev model can provide a possible explanation of the sawtooth-period enhancement with gas-puff as follows: the observed increase of the core-temperature results in a delay in current penetration for the sawtooth cycle initiated after the crash of the pre-gas-puff cycle, and it delays the onset of the $m=1$ mode [28]. Moreover, the growth rate of the $m=1$ mode decreases as the core-temperature increases. A combination of these two effects may result in the sawtooth period extension. However, the amplitude of the $m=1$ oscillations at the crash time is observed to be random irrespective of whether the crash occurs with or without gas pulse. The persistence of these oscillations observed in Figure 6d at the onset as well as after the crash indicates that resistive reconnection may not be related to the internal disruption in our scenario [29]. In the present experiment, the sawtooth inversion takes place around the radius $\rho \sim 0.2$ (the $q=1$ surface), regardless of the presence or absence of the gas puff (see Figure 8). As the density remains flat inside this radius, the temperature profile determines the pressure profile there. The T_e profiles just before and after the crash are shown in Figure 7a. The profile certainly become flattened after the crash in both cases. To investigate the change in inverse T_e scale length, $1/L_{Te} (= -dT_e/T_e dr)$ with time at $\rho \sim 0.2$, $1/L_{Te}$ is plotted in Figure 7b at three different time intervals from the beginning to the end of the sawtooth period, for both with and without gas-puff cases. Each data point in the figure represents an average of tens of sawtooth cycles, with error bars representing the scatter in the measurements.

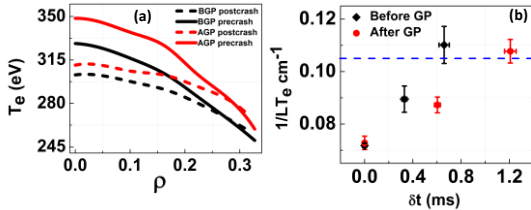


Fig.7. (a) T_e profile at the core at pre and post sawtooth crash time with and without gas pulse injection. (b) represents the threshold of $1/L_{Te}$ value at ($\rho \sim 0.2$) to occur a sawtooth crash.

Interestingly, sawtooth crashes take place around $1/L_{Te} \sim 0.11$ for all cycles, regardless of gas puff being present or not. The observation strongly points towards a threshold for the temperature gradient at the inversion radius that relates to the crash. The Ohmic heating and heat loss rates determine the evolution of T_e profile near the inversion radius during the ramp phase of a new sawtooth cycle. The current diffusion time in the core area is substantially long (~ 30 ms). So, the Ohmic power remains almost unchanged over sawtooth cycles before and after gas-puff. Then, it is the heat transport from the core region that determines the temperature gradient.

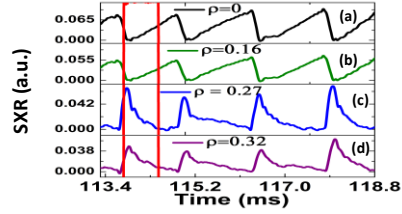


Figure 8: SXR intensity time traces from different chords: $\rho = 0, 0.16, 0.27, 0.32$, showing sawtooth and inverted sawtooth (vertical lines indicate time of gas-puff pulse)

The reduced heat diffusivity with the gas-puff is experimentally demonstrated in Figure 8, which displays the time traces of SXR intensity for chords $\rho = 0, 0.16, 0.27$ and 0.32 . The observed SXR emission inverts its character outside $\rho \sim 0.2$ (the inversion radius), i.e. after a sawtooth crash inside it increases sharply outside. This indicates sudden heat pulse propagation outwards. The SXR intensity returns to the pre-crash value within $500 \mu\text{s}$ for the case of no gas injection, whereas, it takes longer time $\sim 1000 \mu\text{s}$ with gas-puff (Figure 8c and 8d), suggesting reduced heat diffusivity. A plausible explanation is that the reduction in TEM-induced heat diffusivity in the core region by gas-puff delays the attainment of the critical T_e gradient, thereby, prolonging the sawtooth ramp-time.

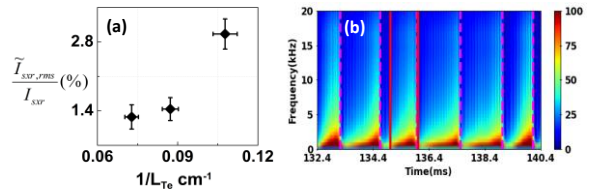


Fig.9.(a) RMS value of SXR intensity fluctuation as a function of inverse T_e scale length at $\rho=0$.(b) The CWTM of SXR intensity fluctuation before and after GP (solid vertical lines). Dashed vertical lines show the time of sawtooth crash.

From Figures 4b and 7b it is evident the local T_e gradient increases as sawtooth develops. In Figure 9a, the amplitude of the SXR intensity fluctuation is plotted against $1/L_{Te}$ at $\rho \sim 0.2$. As the T_e profile steepens, that is, as $1/L_{Te}$ increases, the fluctuation amplitude is seen to increase slowly. But at a critical value of $1/L_{Te}$ the amplitude increases sharply and the crash follows. Interestingly, continuous morlet2 wavelet transform (CWTM) analysis [30] of the central chord SXR intensity, (Figure 9b) indicates development of a broadband turbulence in the core temperature just before the crash which reduces considerably after the crash. So, it seems the sawtooth crash may be triggered by development of a broadband turbulence in core T_e when a critical value of $1/L_{Te}$ is reached [13, 23] at the $q=1$ surface. In conclusion, the present experiments in ADITYA-U tokamak demonstrated that edge-injected short gas-puff pulse could be a novel way of controlling

sawtooth relaxation. Without gas puff, the sawtooth ramp crashes shortly following the appearance of the $m=1$ mode, though the oscillations last even afterwards. After a gas-puff, outside of the core region undergoes an electron density rise within 1 ms, flattening the density profile, which suppresses the TEM modes and reduces heat transport. In contrast, it raises the core temperature later within the $q=1$ surface ($\rho \sim 0.20$) making the profile steeper. The sawtooth crash is seen to occur when a critical temperature gradient ($1/L_{Te} \sim 0.11$) is reached near the inversion radius ($\rho \sim 0.2$) irrespective of gas-puff or not [24]. A sharp rise of a broadband turbulence at this gradient seems relevant to the sawtooth crash. Reduced heat transport with gas injection delays attaining this critical gradient. The observed gas-puff-induced temperature profile variation influences the sawtooth cycle similar to those observed due to localized ECR heating experiments near $q=1$ surface. This new technique, therefore, provides an alternative and relatively simpler method for in-depth study of sawtooth phenomena in tokamaks without facing the complexities of external heating.

References:

- [1] S. von Goeler, W. Stodiek, and N. Sauthoff, Studies of Internal Disruptions and $M=1$ Oscillations in Tokamak Discharges with Soft—X-Ray Techniques, *Phys. Rev. Lett.* **33**, 1201 (1974).
- [2] G. L. Jahns, M. Soler, B. V. Waddell, J. D. Callen, and H. R. Hicks, Internal Disruptions in Tokamaks, *Nucl. Fusion* **18**, 609 (1978).
- [3] O. Sauter et al., Control of Neoclassical Tearing Modes by Sawtooth Control, *Phys. Rev. Lett.* **88**, 4 (2002).
- [4] D. Liu, W.W. Heidbrink et al, Effect of sawtooth crashes on fast ion distribution in NSTX-U; *Nucl. Fusion* 58(2018) 082028
- [5] M. F. F. Nave et al., Role of Sawtooth in Avoiding Impurity Accumulation and Maintaining Good Confinement and Maintaining Good Confinement in JET Radiative Mantle Discharges, *Nucl. Fusion* **43**, 1204 (2003).
- [6] J.A. Wesson; Sawtooth reconnection; 1990 *Nucl. Fusion* 30 2545
- [7] F. Porcelli, D. Boucher, and M. N. Rosenbluth, Model for the Sawtooth Period and Amplitude, *Plasma Phys. Control. Fusion* **38**, 2163 (1996).
- [8] D. J. Campbell et al., Stabilization of Sawteeth with Additional Heating in the JET Tokamak, *Phys. Rev. Lett.* **60**, 2148 (1988).
- [9] I. T. Chapman, Controlling Sawtooth Oscillations in Tokamak Plasmas, *Plasma Phys. Control. Fusion* **53**, (2011).
- [10] I. T. Chapman, T. C. Hender, S. Saarelma, S. E. Sharapov, R. J. Akers, and N. J. Conway, The Effect of Toroidal Plasma Rotation on Sawteeth in MAST, *Nucl. Fusion* **46**, 1009 (2006).
- [11] J. P. Graves, R. J. Hastie, and K. I. Hopcraft, Effects of Sheared Toroidal Plasma Rotation on the Internal Kink Mode in the Banana Regime, *Plasma Phys. Control. Fusion* **42**, 1049 (2000).
- [12] S. Tanaka et al., Sawtooth Stabilization by Electron Cyclotron Heating at the $q=1$ Surface in the WT-3 Tokamak, *Phys. Fluids B* **3**, 2200 (1991).
- [13] G. Wang et al, Core electron temperature turbulence and transport during sawtooth oscillations in the DIII-D tokamak; *Nucl. Fusion* 64 (2024) 066024
- [14] T. Macwan, H. Raj, K. Singh, S. Dolui, and E. Al, Gas-Puff Induced Cold Pulse Propagation in ADITYA-U Tokamak, *Nucl. Fusion* **61**, (2021).
- [15] P. Rodriguez-Fernandez, C. Angioni, and A. E. White, Local Transport Dynamics of Cold Pulses in Tokamak Plasmas, *Rev. Mod. Plasma Phys.* **6**, 1 (2022).
- [16] D. R. Baker, Density Profile Consistency, Particle Pinch, and Cold Pulse Propagation in DIII-D, *Phys. Plasmas* **4**, 2229 (1997).
- [17] R. T. Snider; Modification of sawteeth by second harmonic electron-cyclotron heating in a tokamak; *Phys. Fluids B* **1**, 404–413 (1989)
- [18] R. L. Tanna and S. et al., Ghosh, J....Dolui, Overview of Recent Experimental Results from the ADITYA-U Tokamak, *Nucl. Fusion* **62**, (2022).
- [19] U. Nagora, A. Sinha, S. K. Pathak, P. Ivanov, R. L. Tanna, K. A. Jadeja, K. M. Patel, and J. Ghosh, Design & Development of 140 GHz D-Band Phase Locked Heterodyne Interferometer System for Real-Time Density Measurement, *J. Instrum.* **15**, 0 (2020).
- [20] F. C. JAHQDA; Continuum Radiation in the X Ray and Visible Regions from a Magnetically Compressed Plasma (Scylla); *PHYSICAL REVIEW VOLUME* 119, NUMBER 3
- [21] J Raval et al, “Development Of Multipurpose Soft X-Ray Tomography System For Aditya-U”, https://conferences.iaea.org/event/151/papers/6384/files/4690fec2018_preprint_jayesh_rava_p4_18.pdf, Preprint, FEC 2018, in (n.d.).
- [22] K.Singh,S.Dolui et al.;MHD activity induced coherent mode excitation in the edge plasma region of ADITYA-U tokamak; *Phys. Plasmas* 31, 092511 (2024)
- [23] Y Y Xie et al, Suppression of core temperature fluctuations by edge cooling in the J-TEXT tokamak ; *Plasma Phys. Control. Fusion* 67 015008
- [24] T. Singh, D. Sharma, T. Macwan, S. Sharma, J. Ghosh, A. Sen, Z. Lin, and A. Kuley, Gyrokinetic Simulations of Electrostatic Microturbulence in ADITYA-U Tokamak, *Nucl. Fusion* **63**, (2023).
- [25] Deepti Sharma et al, Aditya Upgradation – Equilibrium study; *Fusion Engineering and Design*
- [26] P. Rodriguez-Fernandez et al., Predict-First Experiments and Modeling of Perturbative Cold Pulses in the DIII-D Tokamak, *Phys. Plasmas* **26**, (2019).
- [27] M. N. Bussac and R. Pellat, *Phys. Rev. Lett.* **59**, 2650(198)
- [28] H. R. Koslowski, H. Soltwisch, and W. Stodiek, Polarimetric Measurement of $m = 1$ Sawtooth Precursor Oscillations in the TEXTOR Tokamak, *Plasma Phys. Control. Fusion* **38**, 271 (1996).
- [29] T.K. Chu, Effect of reconnection of magnetic field lines and electron thermal conduction on the plasma pressure gradient in a sawtooth oscillation, 1988 *Nucl. Fusion* 28 1109
- [30] Brian Russell, and Jiajun Han; Jean Morlet and the Continuous Wavelet Transform
- [31] M. T. Beidler and P. A. Cassak, Model for Incomplete Reconnection in Sawtooth Crashes, *Phys. Rev. Lett.* **107**, 1 (2011)
- [32] A. J. LICHTENBERG; THE ROLE OF STOCHASTICITY IN SAWTOOTH OSCILLATIONS; 1992 *Nucl. Fusion* 32 495